Published in final edited form as:
Bioconjug Chem. 2011 August 17; 22(8): 1479–1483. doi:10.1021/bc2002049.

New covalent capture probes for imaging and therapy, based on a combination of binding affinity and disulfide bond formation

Tolulope A. Aweda, **Vahid Eskandari**, **David L. Kukis**[†], **David L. Boucher**[†], **Bernadette V. Marquez**, **Heather E. Beck**, **Gregory S. Mitchell**[†], **Simon R. Cherry**[†], and **Claude F. Meares**[*]
Chemistry Department, University of California, Davis, CA 95616

[†]Center for Molecular and Genomic Imaging, University of California, Davis, CA 95616

Abstract

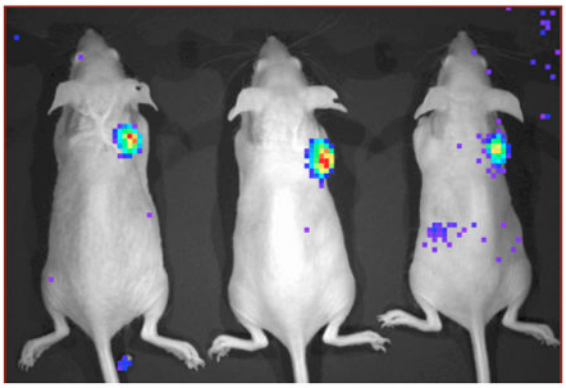

We describe the synthesis and development of new reactive DOTA-metal complexes for covalently targeting engineered receptors *in vivo*, which have superior tumor uptake and clearance properties for biomedical applications. These probes are found to clear efficiently through the kidneys and minimally through other routes, but bind persistently in the tumor target. We also explore the new technique of Cerenkov luminescence imaging to optically monitor radiolabeled probe distribution and kinetics *in vivo*. Cerenkov luminescence imaging uniquely enables sensitive noninvasive *in vivo* imaging of a β^- emitter such as ^{90}Y with an optical imager.

Developing synthetic molecules that specifically target cancer cells is a major goal of biomedical science. Among the most promising approaches are those based on affinity for a molecular target prominently displayed on the target cells, such as the RGD peptides for binding to cell surface integrins,[1] or the somatostatin analog octreotide for binding to type 2 somatostatin receptors.[2] This strategy may be complemented by the development of molecules with connector functions that link selectable sites of disease *in vivo* to validated probes, such as the widely used synthetic DOTA-metal complexes. Though there are variations, such connector molecules usually are engineered proteins derived from antibodies and are useful for "pretargeting," where the connector is administered before the probe.[3, 4] An example is the streptavidin-scFv fusion proteins used as connectors for pretargeted imaging and therapy, along with biotin-tagged DOTA-metal probes possessing

[*]Address correspondence to Claude F. Meares, Chemistry Department, University of California, Davis, CA 95616. cfmeares@ucdavis.edu; phone 530-752-0936; fax 530-752-8938.

Supporting Information Available: Experimental details for all syntheses and experimental methods. This material is available free of charge via the Internet at http://pubs.acs.org.

optimized biodistribution properties.[5] An alternative to the biotin-streptavidin system is infinite affinity probe capture using an engineered binding site that forms a stable covalent bond to the probe.[6] When formulated using a humanized antibody, the latter system presents fewer concerns about protein immunogenicity than streptavidin. Altering the cell-binding moiety of the connector protein while retaining the probe-binding receptor should make it practical to image a choice of biological targets with the same small probe molecule. Other approaches related to pretargeting include the dock-and-lock technique,[7] and a tetrazine/ trans-cyclooctene cycloaddition strategy.[8]

Previously we engineered an antibody into a specific DOTA probe-binding receptor site, with a cysteine side chain placed for permanent probe capture.[9, 10] Wei et al. have inserted this into reporter gene DAbR1 and demonstrated its favorable probe-capture properties in an animal model (Figure 1A).[11] Here we consider changes in the structure and function of the synthetic DOTA probe, to further improve its biodistribution properties. Our prior work employed Michael addition of the cysteine thiol to an acrylamide side chain on the AABD(Y) probe, here denoted as **1**-Y (Figure 1C).[9, 10] This reaction is clean and efficient *in vivo* and forms a stable thioether bond between probe and receptor, but clearance of the free probe occurs significantly through both the urinary and the slower intestinal route,[11] delaying removal of uncaptured probe from the organism. With the goal of identifying new probes that clear efficiently through the kidneys and minimally through other routes, we considered thiol-disulfide interchange, which has several features that allow manipulation of the probe's properties *in vivo*.

The DAbR1 tumor model system described by Wei et al.[11] provides an excellent starting point for testing the properties of candidate probe molecules *in vivo*. Because of the abundance of the free thiol form of the essential cysteine demonstrated for U-87 glioma expressing the DAbR1 reporter,[12] we chose to explore probes such as **5**-^{90}Y carrying the disulfide group as replacements for the electrophilic acryloyl group. This chemistry involves displacement of the leaving group RSH after the probe binds to the receptor, forming a new disulfide bond between the probe and the engineered cysteine on the protein. A motivation for changing from Michael addition to thiol-disulfide interchange was that if any probe-receptor conjugates are taken into endosomes inside cells, the disulfide bond between protein and probe is likely to be reduced and cleaved, releasing the probe and lessening concerns about triggering an immune response.

To implement the use of thiol-disulfide chemistry, it is necessary to address several points. The disulfide group on the new class of probes reacts only with thiols under physiological conditions, but this raises the question whether it would tag naturally occurring thiols in the body such as Cys-34 on albumin; what's more, it is possible that any such potential side reactions would be influenced by the nature of the side chain R in Figure 1C,D. A separate concern is that a disulfide linkage to receptor DAbR1 might prove less stable *in vivo* than the thioether linkage; if so, this could diminish the advantage of covalent bond formation.

Another consideration is that the side chain R might be varied to modify the clearance properties of the probe, for example by increasing its hydrophilicity, in addition to adjusting the reactivity of the probe's disulfide group. The structure of the parent protein-probe complex from which DAbR1 was designed shows that the DOTA moiety of the probe interacts directly with the protein, while the probe's side chain protrudes into solution (Figure 1B).[13] This gives rise to the further possibility that a branched side chain can be introduced in order to add additional functions, such as a carbohydrate group to modify biodistribution.[14] Here we report the first studies exploring these questions, using the new technique of Cerenkov luminescence imaging to optically monitor radiolabeled probe distribution and kinetics *in vivo*.[15] Cerenkov luminescence imaging uniquely enables

sensitive noninvasive *in vivo* imaging of a β^- emitter such as ^{90}Y, and offers informative qualitative images with relatively simple instrumentation.

Multimodal DAbR1-2A-mCherry Reporter Gene and Stable Expression in U-87 Glioma Cells

DNA sequences encoding the DAbR1 and mCherry reporter genes were subcloned to a lentiviral expression vector and linked by sequence encoding a 2A "self-cleaving" peptide to enable bicistronic expression of both reporter genes driven by a single CMV promoter. U-87 glioma cells were exposed to lentiviral particles delivering the basic reporter / selectable marker expression cassette to establish the U-87/DAbR1-2A-mCherry, or U-87/DC cell line. This cell line was then used for paired injections into the subscapular region of SCID Hairless Outbred (SHO) mice, with U-87/DC injected to the right shoulder and the parental U-87 line injected to the left shoulder. Details are provided in Supporting Information.

Probe Synthesis and Imaging

Prior to introduction of radiolabeled probe, mice were imaged on a Maestro 2 (Cambridge Research and Instrumentation) to verify fluorescent mCherry (and indirectly DAbR1) expression in U-87/DC derived tumors (Figure 2A). The new probes were synthesized as outlined in Scheme 1 and radiolabeled with ^{90}Y by the methods detailed in Supporting Information. Probes (8 μCi in 100 μL total volume) were administered via tail vein injection to mice sedated with 2% isoflurane. Following administration, Cerenkov luminescence images of the ^{90}Y distributions were acquired dynamically for a period of 45 min—Figure 2B shows the image acquired beginning at 9 min post injection on an IVIS 100 system (Caliper Life Sciences)—after which time the mice were awakened and returned to their cage. Cerenkov images were acquired again at 1.5 and 3.5 h post injection (Figures 2C and 2D).

Images

As shown in Figure 2, tail-vein injection of **5b**-^{90}Y in 3 animals led to clear visualization of the U-87 tumor on the right shoulder, harboring the DAbR1 gene. A matching tumor on the left shoulder lacked this gene and was not visualized. Parallel results were observed *in vivo* with the homologous probe **5a**-^{90}Y. Uncaptured probes cleared almost exclusively through the kidney, leading to excellent tumor/background ratios one to two hours after injection.

Biodistributions

To address whether the disulfide bond formed between the DAbR1 receptor and either of the **5**-^{90}Y probes persists *in vivo*, biodistributions were carried out 48 h after probe injection. Results are plotted in Figure 3. Even at 48 h, both **5**-^{90}Y probes show excellent concentration in tumor (6.3±2.1 %/g for **5b**-^{90}Y; 14.4±4.5 %/g for **5a**-^{90}Y; $p<0.05$). The kidneys showed highest normal organ uptake (0.38±0.03 %/g for **5b**-^{90}Y; 1.71±0.19 %/g for **5a**-^{90}Y; $p<0.05$); all other organs were <0.2 %/g. Both **5**-^{90}Y probes persist in the tumor to a degree that compares favorably with **1**-^{90}Y (see below), implying that the attachment to DAbR1 is stable *in vivo*. This stability may be related to the noncovalent binding affinity of probe for receptor ($K_D=2\times10^{-9}$ M),[12] which facilitates the specific disulfide bond formation. Note that without covalent attachment, the dissociation of similar probes from DAbR1 occurs with a half-life of ≈100 sec.[12]

It is notable that side reactions with the free cysteine side chain on the abundant (0.5 mM) albumin molecules in circulation evidently did not occur to a significant degree. Part of the reason for this may be that the disulfide bonds in **5a** or **5b** are not activated in the way that

disulfide bonds are when they contain the familiar thiopyridine or thionitrobenzoate leaving groups, so there is little thermodynamic driving force to propel thiol-disulfide interchange between molecules diffusing freely in solution. On the other hand, after the reversible probe-receptor complex has been formed, release of the RSH leaving group (Figure 1D) may be entropically favorable due to the extra translational and rotational degrees of freedom created by this process.[16] Thiol-disulfide interchange between the probes and small thiols may be more difficult to detect, but the significant differences between the biodistributions of **5a**-^{90}Y and **5b**-^{90}Y suggest that interchange between these probes and small thiols are not important, since that would tend to make the probe distributions similar. For example, if both probes rapidly reacted with free cysteine in circulation and lost their original leaving groups, we would expect their biodistributions to be identical.

Previously Wei et al. used a related model system, finding 24 h tumor uptake of **1**-^{90}Y was 4.9±0.6 %/g. Other organs showed some uptake of **1**-^{90}Y at 24 h, notably spleen (1.3±0.5 %/g), liver (0.8±0.3 %/g), and small intestine (0.3±0.3 %/g); bone uptake was a satisfactory 0.2±0.1 %/g.[11] In contrast to **1**-^{90}Y, the **5**-^{90}Y probes exhibit very little residue in spleen, liver, or intestine; instead, they show modestly higher kidney uptake. This is corroborated by the Cerenkov images, which imply clearance mainly through the kidney with very little through the liver and intestines. It is interesting to note that the **5b**-^{90}Y probe shows significantly lower concentration in both tumor and kidney than **5a**-^{90}Y (Figure 3). While the cause requires more investigation, it may be that compared to the acetate group of **5a**, the bulkier propionate group of **5b** reduces the accessibility of the disulfide bond. Further explorations of alternative leaving groups may refine the properties of this family of probes.

Time scale for target visualization

As shown in Figure 2, substantial tumor uptake occurs within a few minutes, and background clears within a few hours. This is a highly favorable set of results that suggests, for example, that glucose might be replaced by 2-[^{18}F]fluorodeoxyglucose for PET imaging on this time scale. On the other hand, the very long persistence in the target indicates stable attachment of the probe to the receptor, which would be favorable for multi-day procedures such as targeted radiotherapy with ^{90}Y.[5] While imaging requires good target/background ratios, preferably at short times, therapy benefits from long residence times of the radiopharmaceutical on the target, for the delivery of the maximum radiation dose. The therapeutic radionuclide ^{90}Y decays with a physical half-life of 64 h, making it advantageous to bind a probe such as **5**-^{90}Y on the target for at least that long; permanent binding is excellently suited for this application.

Supplementary Material

Refer to Web version on PubMed Central for supplementary material.

Acknowledgments

Imaging and animal expenses were supported in part by NIH research grant CA143098 (SRC). Chemical synthesis was supported in part by NIH research grants CA016861 (CFM) and CA136639 (CFM). Jennifer Fung and Michelle Connell, Center for Molecular and Genomic Imaging, UC Davis, provided technical support for the imaging studies.

Literature Cited

1. Liu S. Radiolabeled Cyclic RGD Peptides as Integrin alphavbeta3-Targeted Radiotracers: Maximizing Binding Affinity via Bivalency. Bioconjugate Chem. 2009; 20:2199–2213.

2. Maresca KP, Marquis JC, Hillier SM, Lu G, Femia FJ, Zimmerman CN, Eckelman WC, Joyal JL, Babich JW. Novel Polar Single Amino Acid Chelates for Technetium-99m Tricarbonyl-Based Radiopharmaceuticals with Enhanced Renal Clearance: Application to Octreotide. Bioconjugate Chem. 2010; 21:1032–1042.

3. Goodwin DA, Meares CF, Watanabe N, McTigue M, Chaovapong W, Ransone CM, Renn O, Greiner DP, Kukis DL, Kronenberger SI. Pharmacokinetics Of Pretargeted Monoclonal Antibody 2D12.5 And Y-88-Janus-2-(p-Nitrobenzyl)-1,4,7,10-Tetraazacyclododecanetetraacetic Acid (DOTA) In Balb/c Mice With KHJJ Mouse Adenocarcinoma - A Model For Y-90 Radioimmunotherapy. Cancer Res. 1994; 54:5937–5946. [PubMed: 7954426]

4. Weiden P, Breitz H, Press O, Appelbaum J, Stone D, Bryan K, Su F, Axworthy D, Hylarides M, Theodore L, Beaumier P, Reno J. Radioimmunotherapy (RIT) in the treatment of non-Hodgkins lymphoma (NHL): Advantage of pretargeted RIT (PRITR). Blood. 1998; 92:414A–414A.

5. Press O, Wilbur S, Lin Y, Hamlin D, Gopal A, Pagel J. Conventional and pretargeted radioimmunotherapy of B cell lymphomas using CD20, CD22, and HLA DR as target antigens. Cancer Biotherapy Radiopharm. 2008; 23:522–522.

6. Chmura AJ, Orton MS, Meares CF. Antibodies with infinite affinity. Proc Natl Acad Sci USA. 2001; 98:8480–8484. [PubMed: 11447282]

7. Goldenberg DM, Rossi EA, Sharkey RM, McBride WJ, Chang CH. Multifunctional Antibodies by the Dock-and-Lock Method for Improved Cancer Imaging and Therapy by Pretargeting. J Nucl Med. 2008; 49:158–163. [PubMed: 18077530]

8. Devaraj N, Upadhyay R, Haun JB, Hilderbrand SA, Weissleder R. Fast and Sensitive Pretargeted Labeling of Cancer Cells through a Tetrazine/trans-Cyclooctene Cycloaddition. Angew Chem Intl Ed. 2009; 48:7013–7016.

9. Corneillie TM, Lee KC, Whetstone PA, Wong JP, Meares CF. Irreversible Engineering of the Multielement-Binding Antibody 2D12.5 and Its Complementary Ligands. Bioconjugate Chem. 2004; 15:1392–1402.

10. Corneillie TM, Whetstone PA, Lee KC, Wong JP, Meares CF. Converting Weak Binders into Infinite Binders. Bioconjugate Chem. 2004; 15:1389–1391.

11. Wei LH, Olafsen T, Radu C, Hildebrandt IJ, McCoy MR, Phelps ME, Meares C, Wu AM, Czernin J, Weber WA. Engineered Antibody Fragments with Infinite Affinity as Reporter Genes for PET Imaging. J Nucl Med. 2008; 49:1828–1835. [PubMed: 18927335]

12. Aweda TA, Beck HE, Wu AM, Wei LH, Weber WA, Meares CF. Rates and Equilibria for Probe Capture by an Antibody with Infinite Affinity. Bioconjugate Chem. 2010; 21:784–791.

13. Corneillie TM, Fisher AJ, Meares CF. Crystal structures of two complexes of the rare-earth-DOTA-binding antibody 2D12.5: Ligand generality from a chiral system. J Am Chem Soc. 2003; 125:15039–15048. [PubMed: 14653738]

14. Schottelius M, Rau F, Reubi JC, Schwaiger M, Wester HJ. Modulation of Pharmacokinetics of Radioiodinated Sugar-Conjugated Somatostatin Analogues by Variation of Peptide Net Charge and Carbohydration Chemistry. Bioconjugate Chem. 2005; 16:429–437.

15. Robertson R, Germanos MS, Li C, Mitchell GS, Cherry SR, Silva MD. Optical Imaging of Cerenkov Light Generation from Positron-Emitting Radiotracers. Phys Med Biol. 2009; 54:N355–365. [PubMed: 19636082]

16. Page MI, Jencks WP. Entropic Contributions to Rate Accelerations in Enzymic and Intramolecular Reactions and Chelate Effect. Proc Natl Acad Sci USA. 1971; 68:1678–1683. [PubMed: 5288752]

17. Day JJ, Marquez BV, Beck HE, Aweda TA, Gawande PD, Meares CF. Chemically modified antibodies as diagnostic imaging agents. Current Opinion in Chemical Biology. 2010; 14:803–809. [PubMed: 20952245]

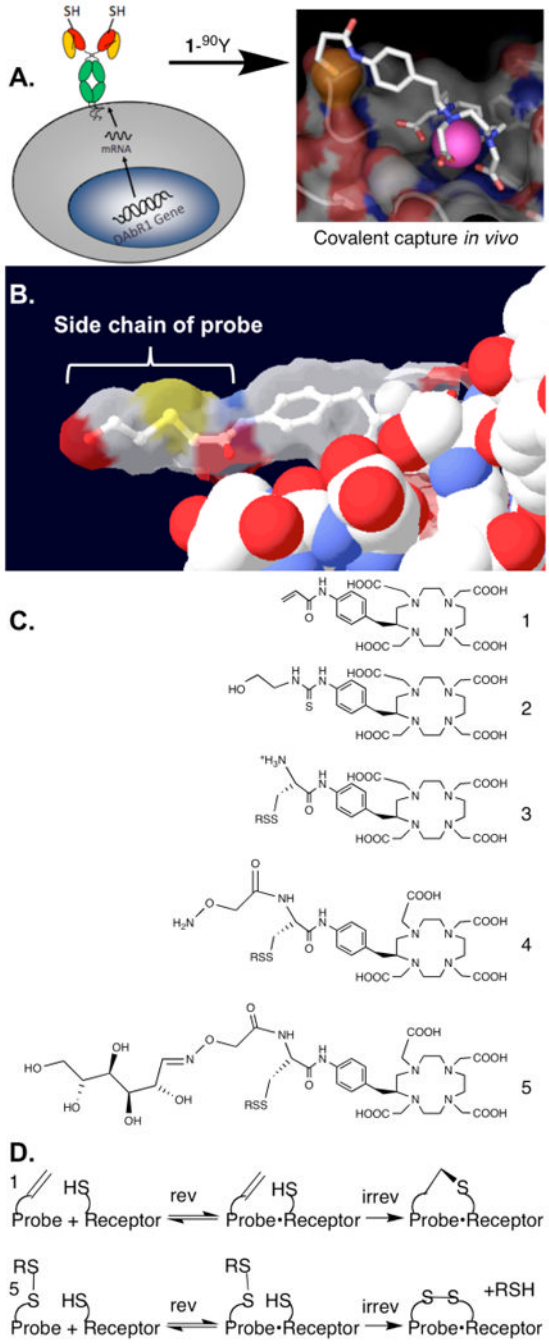

Figure 1.

(A) Flow chart illustrating irreversible probe capture. First the receptor is placed on the surface of a target cell, either by transfection of the receptor gene as shown,[11] or by pretargeting with a bispecific molecule[5]; then the receptor captures the probe **1**-^{90}Y to form a reversible complex, which converts to a stable covalent complex (see 1D below). The pink sphere in the probe structure represents the chelated ^{90}Y. Modified from ref[17] with permission. (B) From PDB file 1NC2,[13] the structure of compound **2**-Y bound to monoclonal antibody 2D12.5, from which the engineered receptor DAbR1 was derived; this shows the lack of interaction between the antibody (solid spacefill) and the side chain of the probe (stick model inside transparent molecular surface), suggesting that the complex will

accommodate probes with a variety of side chain shapes and sizes. For orientation, the benzene ring of **2**-Y can be compared to the benzene ring of **1**-^{90}Y in 1A. (C) Probe structures discussed here, before metal is added. See Scheme 1 for the structures of group R. (D) Comparison of Michael addition of probe **1**-^{90}Y with thiol-disulfide interchange of probe **5**-^{90}Y. Presumably the latter reaction occurs *in vivo* as shown by the results in Figure 2.

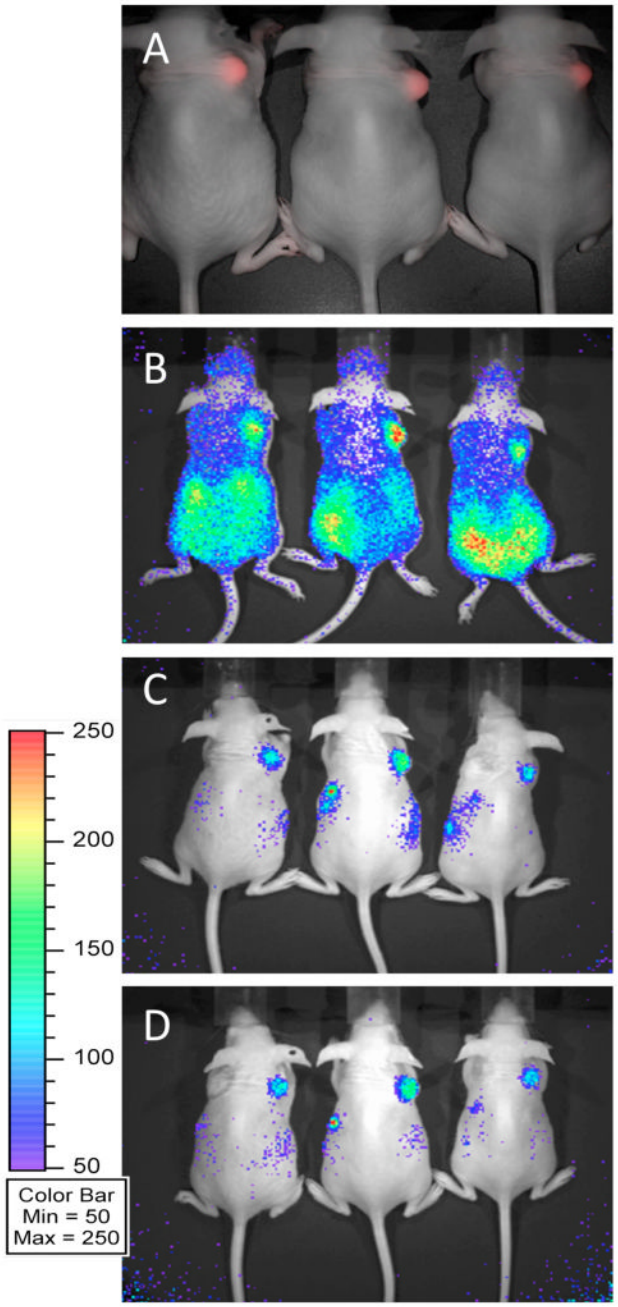

Figure 2.

In vivo imaging of **5b**-^{90}Y. (A) Spectrally unmixed fluorescent image (overlaid with the corresponding monochrome image) acquired for three mice, each of which received bilateral injections of 3×10^6 U-87 glioma cells to the scapular region. Tumors on right shoulders are derived from U-87/DC cells engineered to express DAbR1 and the fluorescent protein mCherry. There are also tumors on the left shoulders, derived from parental U-87 cells without the reporter gene. (B, C & D) Cerenkov luminescence images acquired following tail vein injection of 8 μCi **5b**-^{90}Y. The color scale units (common to B, C, & D) indicate counts per pixel. Images were acquired at B) 9 min, C) 1.5 h and D) 3.5 h post-injection. Similar images were obtained for **5a**-^{90}Y. The color scale units common to B, C, & D

indicate counts per pixel, and correspond to the radiance range $3.4\times10^3 – 1.7\times10^4$ photons/s/cm^2/sr.

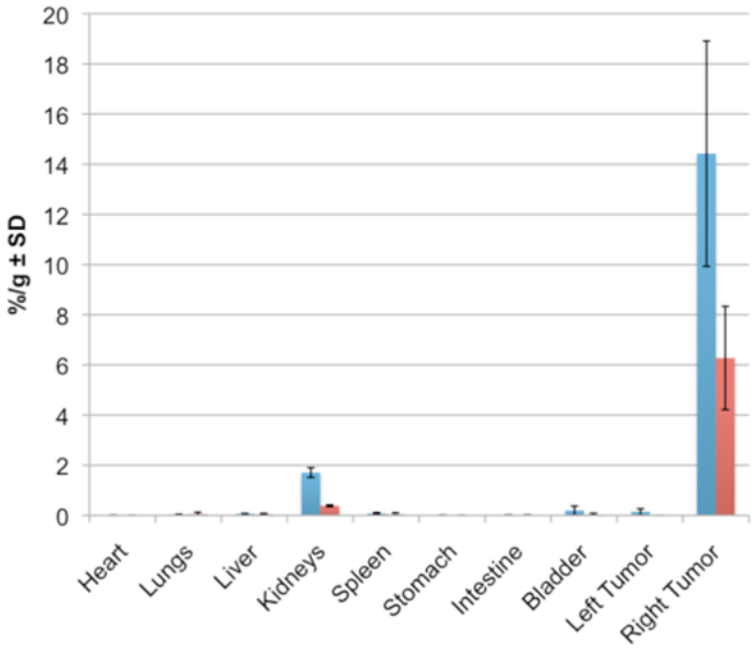

Figure 3.
Mouse biodistributions 48 h after injection of **5a**-^{90}Y (blue) or **5b**-^{90}Y (red). Percent dose per gram tissue ± standard deviation (n=3). See Scheme 1 for structures of **5a** and **5b**. Right tumor expresses the DAbR1 receptor gene.

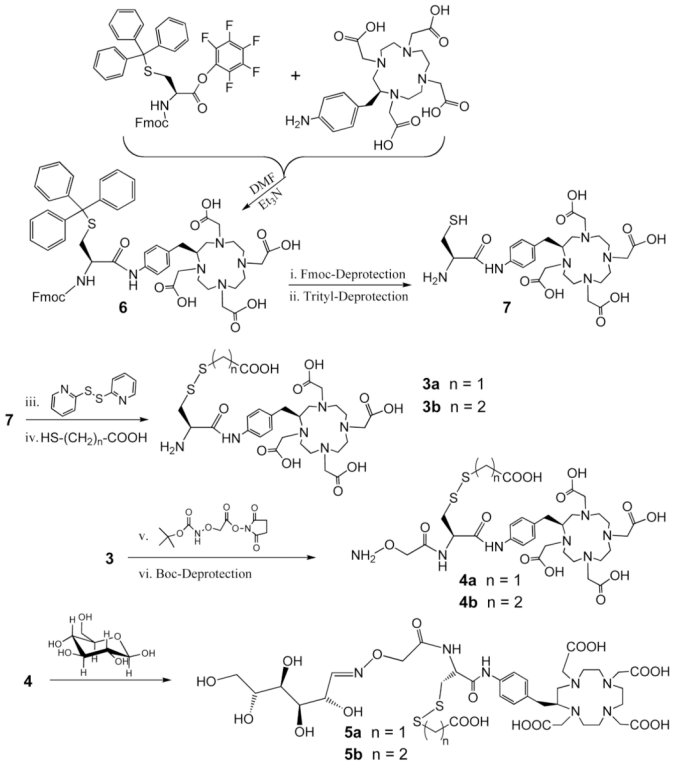

Scheme 1.

Synthesis of new probes. The linear carbohydrate represented for **5** is one of several possible isomers. The leaving group may be selected to improve the biodistribution properties of the probe; e.g., **5a** and **5b** differ by $–CH_2–$ in the R group that is lost by displacement when the probe attaches to the DAbR1 receptor as shown in Figure 1D. Synthesis details are provided in Supporting Information.